Water Science & Technology

IWA PUBLISHING

Water Science & Technology Vol 87 No 11, 2806 doi: 10.2166/wst.2023.166

Hydrophobic modification of a PVDF hollow fiber membrane by plasma activation and silane grafting for membrane distillation

Qiaoru Jin[a,b,†], Xue Zhang[a,†], Fuzhi Li[a] and Xuan Zhao[a,*]

[a] Lab of Environmental Science & Technology, INET, Tsinghua University, Beijing 100084, China
[b] School of Environmental Science & Engineering, Suzhou University of Science and Technology, Suzhou 215009, China
*Corresponding author. E-mail: zhxinet@tsinghua.edu.cn
†Q.J. and X.Z. are co-first authors.

ABSTRACT

Polyvinylidene fluoride (PVDF) hollow fibers were hydrophobically modified using a simple and scalable method of plasma activation and silane grafting. The effects of plasma gas, applied voltage, activation time, silane type, and concentration were investigated according to the membrane hydrophobicity and direct contact membrane distillation (DCMD) performance. Two kinds of silane were used, including methyl trichloroalkyl silane (MTCS) and 1H,1H,2H,2H-perfluorooctane trichlorosilane silanes (PTCS). The membranes were characterized by techniques such as Fourier transform infrared (FTIR), scanning electron microscopy (SEM), X-ray photoelectron spectroscopy (XPS), and contact angle. The contact angle of the pristine membrane was 88°, which increased to 112°–116° after modification. Meanwhile, the pore size and porosity decreased. In DCMD, the maximum rejection reached 99.95% by the MTCS-grafted membrane, while the flux decreased by 35% and 65% for the MTCS- and PTCS-grafted membranes, respectively. Treating humic acid-contained solution, the modified membrane showed steadier water flux and higher salt rejection than the pristine membrane, and 100% flux recovery was achieved by simple water flushing. This two-step method of plasma activation and silane grafting is very simple and effective to improve the hydrophobicity and DCMD performance of PVDF hollow fibers. However, further study on improving the water flux should be carried out.

Key words: anti-fouling, hydrophobic modification, membrane distillation, plasma treatment, PVDF

HIGHLIGHTS

- Hydrophobic modification of PVDF fibers were carried out by plasma activation and silane grafting.
- The operation conditions were optimized according to hydrophobicity and MD performance.
- The contact angles increased from 88° to 112°–116° after modification.
- The salt rejection increased to 99.95%, while the flux reduced for the modified membranes.
- The modified membrane showed higher resistance to humic acid fouling.

GRAPHICAL ABSTRACT

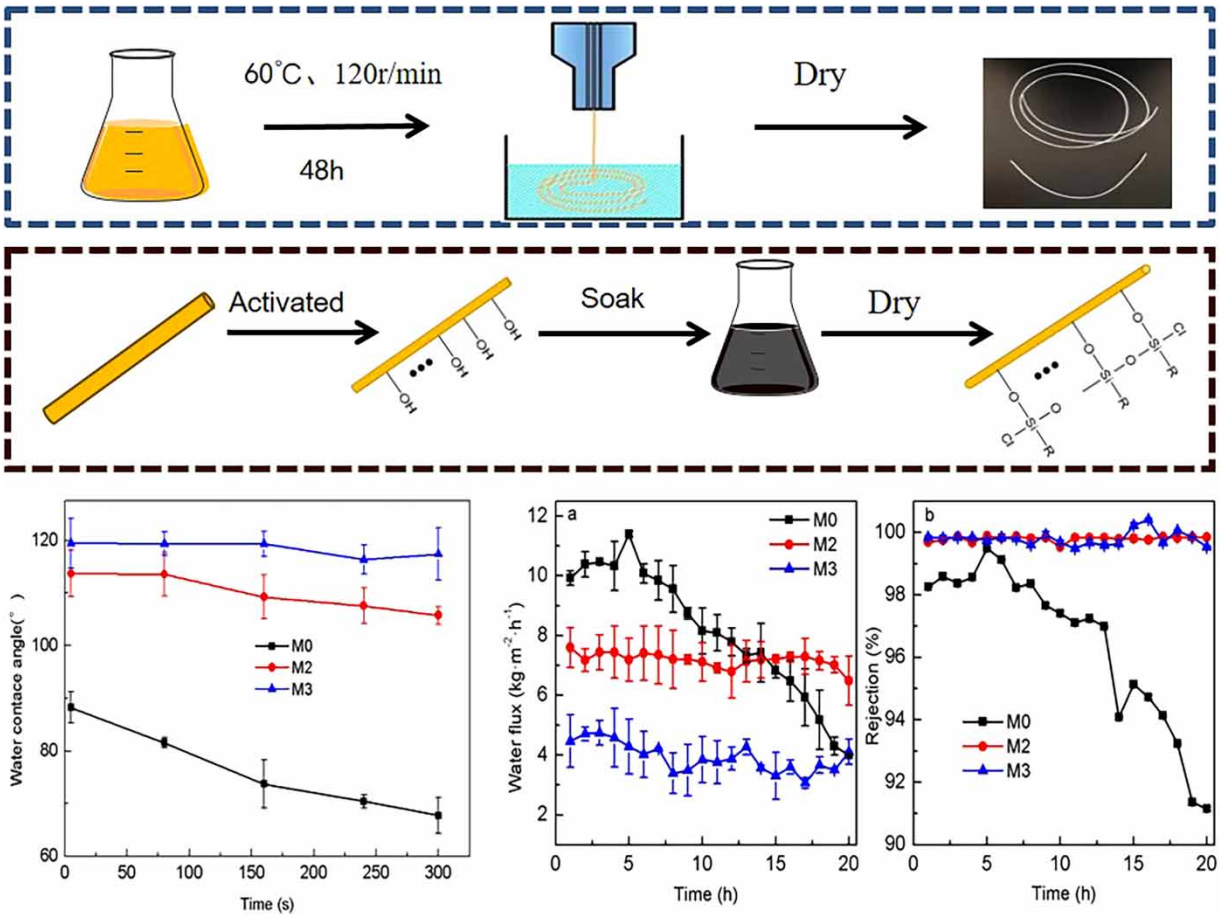

1. INTRODUCTION

As a thermally driven membrane process, membrane distillation (MD) has some advantages, such as lower operating temperature than distillation, lower operation pressure than reverse osmosis, and high rejections of the nonvolatile compounds (Ray *et al.* 2020; Madalosso *et al.* 2021). MD can be applied to treat various wastewater, such as desalination brine, textile wastewater, and oily wastewater (Yan *et al.* 2021). During the MD process, the vapor crosses the microporous hydrophobic membrane while the nonvolatile compounds are kept on the feed side. Thus, the membrane acts as a barrier and plays a vital role in MD efficiency.

Increasing demand for MD technology accelerates the development of hydrophobic membrane fabrication methods, such as 3D imprinting, electrospinning, and attaching nanomaterials (Eykens *et al.* 2017; Ray *et al.* 2020). Water contact angles (WCAs) of the membranes prepared by these methods are generally more than 120° and even up to 160°, and such excellent hydrophobicity enhances the anti-wetting and anti-fouling properties of the membrane (Zhang *et al.* 2017, 2021). However, most of these methods are still in the laboratory. The industrial scaling-up of such membranes seems a long way off. In this study, we will focus on developing a simple and scalable method to prepare hydrophobic membranes.

Among the hydrophobic materials used in the MD process, polyvinylidene fluoride (PVDF) is widely used and outstanding for its high chemical stability, thermal stability, mechanical strength, and feasibility of forming membranes via phase inversion (Kang & Cao 2014; Lee *et al.* 2019). In order to fabricate microporous membranes, some pore-forming additives (e.g., polyvinylpyrrolidone (PVP) and LiCl) are added (Hou *et al.* 2009; Hamzah & Leo 2017). However, these additives remain in the membrane after phase inversion, and enhance the membrane hydrophilicity (Ray *et al.* 2020). The WCAs of such PVDF membranes stay around 90°, which leads to membrane wetting problems during the long-term running (Teoh & Chung 2009).

Besides membrane wetting, membrane fouling is another common problem in the MD process. For example, some natural organic matter (e.g., humic acid and polysaccharide) can easily attach to the membrane surface and pores, causing deterioration of water flux and salt rejection (Hou *et al.* 2015), which is an effective way to enhance membrane hydrophobicity to overcome the fouling and wetting problems (Eykens *et al.* 2017; Mousavi *et al.* 2021). Some commonly used hydrophobic modification methods include electrospinning, coating, chemical vapor deposition, and plasma (Jeong *et al.* 2016; Hamzah *et al.* 2018; Madalosso *et al.* 2021). Of all these methods, plasma treatment is convenient to change the surface properties without influencing the bulk materials, is easy to control, can be repeated, and is environmentally friendly (Boulares-Pender *et al.* 2013; Kravets *et al.* 2022). Plasma treatment always improves surface pore size, porosity, and roughness, and creates hydroxyl groups and other oxygen-containing groups (Gryta 2021a; Madalosso *et al.* 2021). Plasma treatment is always used to enhance surface hydrophilicity (Gryta 2021b; Sharma *et al.* 2021). Thus, further grafting of hydrophobic monomers is necessary to enhance the hydrophobicity (Deng *et al.* 2020).

Fluoroalkyl silanes are known for their low surface free energy with one end of hydrophobic fluoroalkyl, making them suitable hydrophobic monomers (Tran *et al.* 2021; Zhang *et al.* 2021). It is convenient to combine the plasma treatment and silane grafting, which can improve both the porosity and hydrophobicity of the membranes, and eventually improve the MD performance (Yang *et al.* 2011; Xu *et al.* 2015; Liu *et al.* 2016). Many factors, such as plasma activation, silane concentration, and the type of gas may influence the membrane properties (Xu *et al.* 2015; Liu *et al.* 2016; Lee *et al.* 2019).

In this study, hydrophobic modification of the PVDF hollow fiber membrane was carried out using a two-step method of plasma activation and silane grafting. The PVDF hollow fibers were firstly irradiated with plasma and then soaked into the grafting solution. The influence of plasma power, activation time, type of gas, and the silane type and concentration on the membrane hydrophobicity were investigated. Two organosilane monomers were compared, including methyl trichloroalkyl silane (MTCS) and 1H, 1H, 2H, 2H-perfluorooctane trichlorosilane silanes (PTCS). The modified membranes were further characterized for their physicochemical properties and to determine the performance of direct contact membrane distillation (DCMD). The anti-wetting and anti-fouling properties of humic acid were studied during a 20 h running time of DCMD. The possible factors influencing the performance of the modified membrane were then discussed. This hydrophobic modification is simple and scalable, which resulted in higher salt rejection and anti-fouling properties during the MD treatment. However, the permeability should be improved in further study.

2. MATERIALS AND METHODS

2.1. Materials and chemicals

PVDF with a molecular weight of 500 kDa was obtained from Sinochem Blue Sky Fluorine Materials Co., Ltd, China. PVP (k30) was purchased from Sinopharm Chemical Reagent Co., LTD. MTCS and PTCS were purchased from Shanghai McLean Co., Ltd. N,N-dimethylacetamide (DMAc, $>99\%$) and n-hexane were purchased from Rowen Reagent Co., Ltd, China. Humic acid sodium was purchased from Aldrich Reagents. Ultrapure water with conductivity $<2\ \mu S\ cm^{-1}$ and deionized water with conductivity $<10\ \mu S\ cm^{-1}$ were produced by the ultrapure water purification system (Millipore).

2.2. Preparation of the PVDF hollow fiber membrane

The PVDF hollow fiber membrane was prepared by the non-solvent induced phase separation (NIPS) method (Figure 1). The dope solution contained 18 wt% PVDF, 5 wt% PVP, and 77 wt% DMAc. The mixture was placed on the shaker (ZWY-240, Shanghai Zhicheng Inc., China) at 120 rpm at 60 °C for 48 h to get a homogenous solution. The dope solution was then kept still in a constant temperature incubator (BPH-9272, Shanghai Yiheng Inc., China) at 60 °C for another 12 h to degas.

The spinning conditions are shown in Table 1. The homogeneous dope solution of 5 mL was loaded into a syringe and pressed into the spinneret at a flow rate of 6 $mL{\cdot}min^{-1}$. The fibers were soaked in the coagulation bath for 10 min to complete the phase inversion. Then, the fibers were stored in deionized water for 1 day to remove the residual solvent. Finally, the wet fibers were dried at room temperature for the test or further hydrophobic modification.

2.3. Hydrophobic modification of the hollow fiber membrane

The plasma treatment was carried out using a plasma system of PlasmaFlecto 10 (Plasma Technology, Germany). The dry PVDF hollow fibers were placed in the plasma chamber. N_2, O_2, or air gas was introduced into the chamber at 0.5–1 bar after the chamber was vacuumed to 0.2 mbar. After the plasma treatment, the fibers were immediately immersed in the silane solution in a sealed plastic container for 6 h. Silane was dissolved in n-hexane at 0.1–1.0 wt% for grafting. The grafted

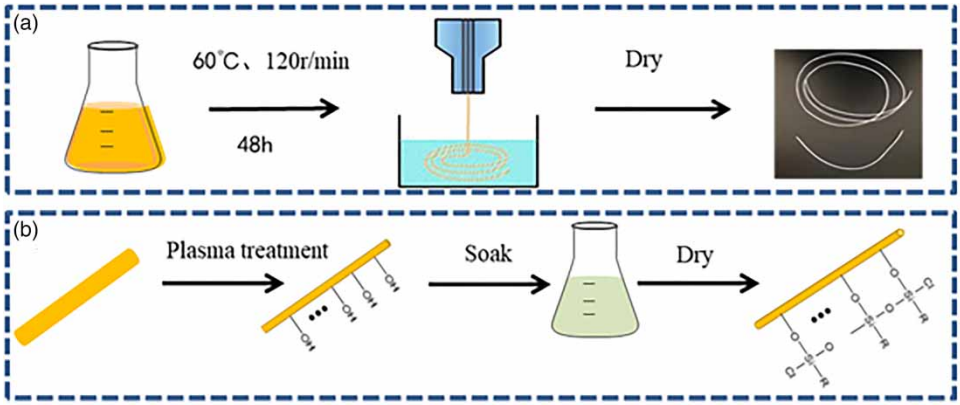

Figure 1 | The schematic diagram of preparation (a) and plasma hydrophobic modification (b) of the PVDF hollow fiber membrane.

Table 1 | Spinning conditions for the PVDF hollow fiber membrane

Parameter	Value
Coagulation bath composition (v/v)	Deionized water/ethanol (9/1)
Coagulation bath temperature (°C)	40
Bore fluid	Ultrapure water
Bore fluid flow rate (mL·min^{-1})	3
Dope solution flow rate (mL·min^{-1})	6
Air gap distance (cm)	10
Spinneret outer diameter (mm)	1.3
Spinneret inner diameter (mm)	0.7

fibers were then rinsed three times with n-hexane to remove any unreacted silane. Finally, the modified fibers were dried at room temperature.

The effects of plasma operation parameters and the silane concentration on the membrane hydrophobicity were investigated in four sets of experiments, as shown in Table 2. After the grafting, the hydrophobicity of the fibers was tested using a WCA. The optimized grafting parameters were chosen based on the hydrophobicity of the modified membranes. Three membrane samples were made using these optimized grafting parameters, including the plasma-treated membrane – M1, MTCS-grafted membrane – M2, and PTCS-grafted membrane – M3. The pristine PVDF membrane was called M0.

2.4. Membrane characterization

The dried membrane was characterized using the following methods. WCA, representing the membrane hydrophobicity degree, was measured by a contact angle goniometer (SL200KS, Kono, America) at 25 °C with ultrapure water drips. The average WCA at five positions was calculated for each membrane sample and the differences between them should be less than 5°. To get the dynamic contact angle, WCAs were recorded every 60 s for a period of 300 s. The functional groups on the membrane surface were measured using a Fourier transform infrared (FTIR) spectrometer (PerkinElmer, USA) with a wavenumber range of 500–4,000 cm^{-1}. Elemental compositions and their states were determined by X-ray photoelectron spectroscopy (XPS, K-alpha, Thermo Scientific, USA) with Al Kα monochromatic source. Surface morphologies were observed via scanning electron microscopy (SEM, Tescan Miran4, Czech) at a magnification of 100,000×. Before SEM observation, the membrane surface was coated with a thin platinum layer at 20 mA for 300 s using an ion sputtering coating device (Q150R ES Plus, Quorum, England). The membrane roughness was measured using atomic force microscopy (AFM, SPM-960, SHIMADZU, Japan) in tapping mode in the air on an area of 10 μm × 10 μm. The average roughness (R_a) and root mean square roughness (R_q) were determined. The pore size and porosity of the fiber were measured by a mercury

Table 2 | Four experiments for the plasma activation and silane grafting condition

	Plasma activation			
Experiment set no.	**Gas**	**Power (w)**	**Time (min)**	**Silane concentration (wt%)**
1	Air N_2 O_2	300	2	1
2	Air	300	0.5 2 4	1
3	Air	150 240 300	2	1
4	Air	300	2	0.1 0.5 1

injection method. The liquid entry pressure of water (LEPw) was estimated by measuring the minimum pressure for the water droplet penetrating the membrane pores. A lab-made equipment was used to test the LEPw (Supplementary material, Figure S1). The tensile strength of the membranes was obtained by a tensile tester (E43, USA) at a loading speed of 20 mm·min^{-1}. The formula for calculating fracture tensile strength is as follows:

$$\sigma = \frac{4F}{(D^2 - d^2)\pi}$$

where σ (MPa) is the tensile strength; F (N) is the fracture tensile strength; D (m) and d (m) are the outer and inner diameters of the hollow fiber, respectively.

2.5. Tests of MD performance

A bench-scale DCMD set-up was used to evaluate the DCMD performance of the membranes M0–M3 (Figure 2). The DCMD module contained 10 fibers with an effective area of 45 cm^2 (Supplementary material, Figure S1). The feed of 20 g·L^{-1} of NaCl solution was heated to 60 °C by a thermostatic system. It was circulated through a diaphragm pump at a flow rate of 0.5 L·min^{-1}. The other side of the module was deionized water, which was kept at 20 °C by a chiller and circulated at a flow rate of 0.3 L·min^{-1}. The DCMD test ran for 8 h. During the test, the water conductivity in the permeate tank was monitored by an online conductivity meter (OHR, China Hongrun Precision Instruments Co., Ltd).

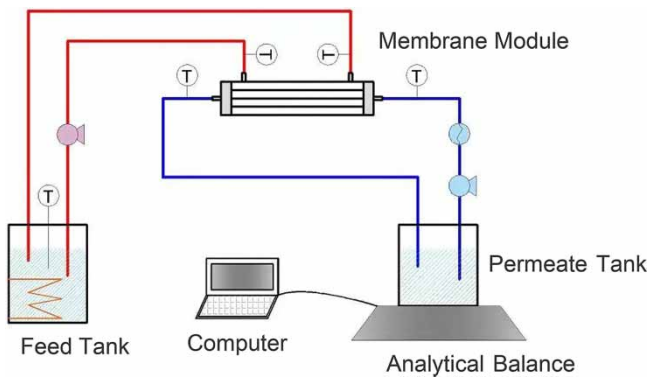

Figure 2 | Schematic representation of the DCMD system.

After 20 g·L^{-1} of NaCl solution was run for an 8-h DCMD test, the feed was replaced to carry on the fouling test. The fouling feed was the solution of 35 g·L^{-1} of NaCl and 30 mg·L^{-1} of humic acid. This test ran for 20 h, and the water flux and salt rejection were recorded. At the end of the test, the feed of the humic acid solution was removed, and the whole system was flushed with deionized water for half an hour. Then 20 g·L^{-1} of NaCl solution was used as the feed and ran for a 3-h DCMD test. The water flux and salt rejection were recorded.

The flux of DCMD was automatically recorded by a digital balance (CP4202C, Ohaus Technologies, USA). The flux (J, kg·m^{-2}·h^{-1}) was determined by the following equation:

$$J = \frac{\Delta W}{A \cdot \Delta t}$$

where ΔW (kg) denotes the weight increase of the permeate tank during the time Δt, A (m^2) is the effective area of the membrane, and Δt is the time duration (h).

The salt rejection (R, %) was calculated as:

$$R = \left[1 - \frac{C_p}{C_f}\right] \times 100\%$$

where C_f (mg·L^{-1}) and C_p (mg·L^{-1}) are the NaCl concentrations in the feed and permeate, respectively. The NaCl concentration in permeate was calculated considering the dilution effect:

$$c_p = \left[\frac{C_t m_t - C_0 m_0}{m_t - m_0}\right]$$

where C_0 (mg·kg^{-1}) and C_t (mg·kg^{-1}) are the NaCl concentrations in the permeate tank at the beginning and time t, m_0 and m_1 are the initial and final masses of permeate stream (kg).

The relative flux recovery ratio (FRR) can be obtained by the following formula (Deng *et al.* 2020):

$$\text{FRR} = \frac{J_c}{J_0} \times 100\%$$

where J_0 (kg·m^{-2}·h^{-1}) is the flux of the unfouled membrane, and J_c is the flux (kg·m^{-2}·h^{-1}) of the fouled membrane after flushing.

3. RESULTS AND DISCUSSION

3.1. Optimization of plasma activation and silane grafting conditions

The effects of the plasma activation and silane grafting conditions on the WCA of the membrane were investigated using four sets of experiments, including gas, plasma treatment time, power, and silane concentration (Figure 3). The WCA of the pristine membrane was 89°, which decreased to 57°–65° after plasma treatment. The membrane with oxygen plasma treatment had the lowest WCA, which may be due to the increasing oxygen-based polar groups in the presence of oxygen (Kawakami *et al.* 2020). Then the WCA increased to 97°–116° after silane grafting. Of all the modified membranes, those treated under air had higher WCAs of 114°–116°, while those treated under oxygen had WCAs under 100° (Figure 3(a)). Maybe the active groups created under the air plasma treatment are more prone to react with silane. Therefore, the plasma treatment was run under air in the following experiments.

As the plasma activation time varied from 0.5 to 4 min, the WCAs of the modified membranes first increased and then decreased (Figure 3(b)). The highest WCAs were obtained at 2 min. Plasma treatment for 0.5–2 min can produce rougher and more porous membrane surfaces, while the 4-min plasma treatment resulted in a less porous surface (Supplementary material, Figure S2). Thus, 2-min plasma treatment was chosen.

With the plasma power varying from 150 to 300 W, the WCAs of the modified membranes slightly increased from 110° to 116° (Figure 3(c)). The effects of plasma power were not significant, and the power of 300 W was used in our following experiments.

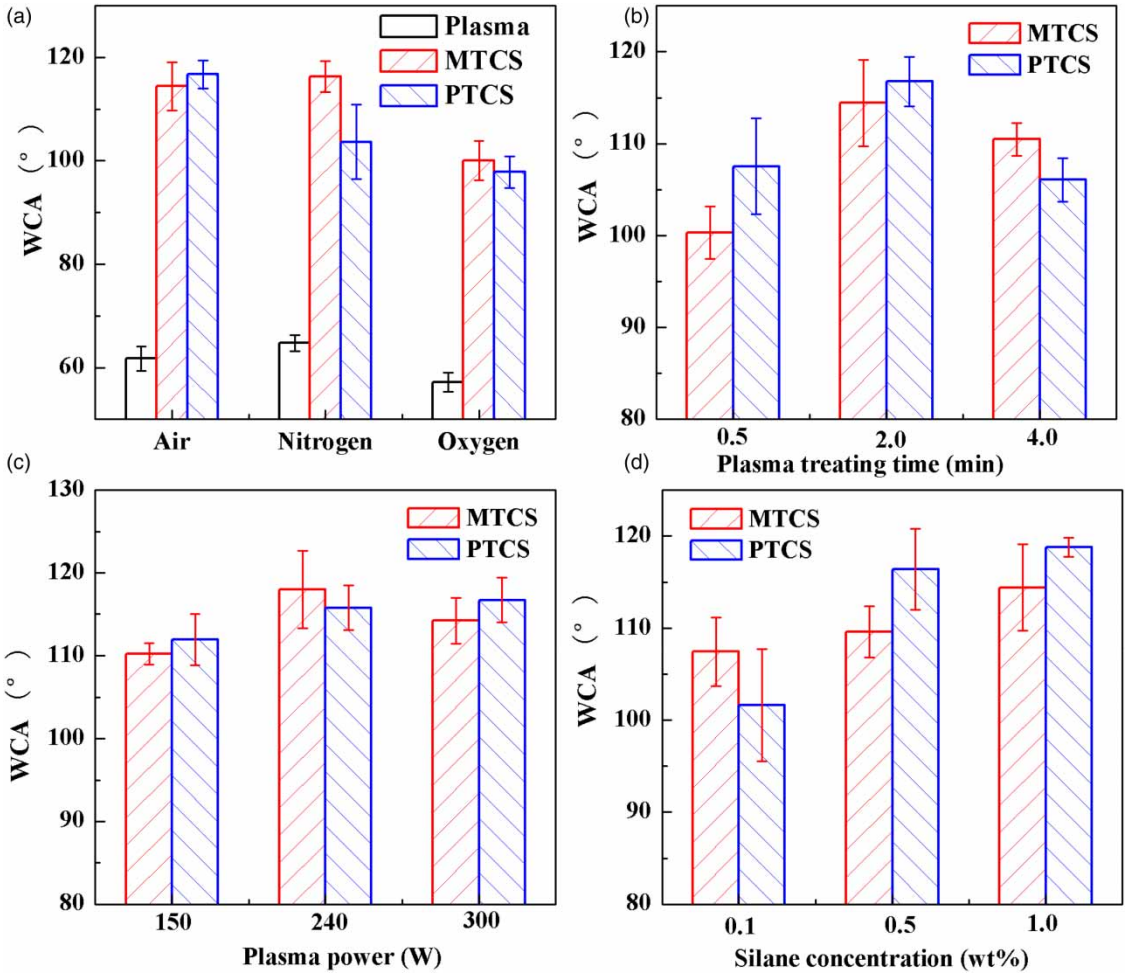

Figure 3 | WCA of the pristine and modified membranes under different gases (a), with different plasma treatment times (b), at different plasma powers (c), and with different silane concentrations (d).

With the silane concentration increasing from 0.1 to 1.0 wt%, the WCAs of the MTCS- and PTCS-grafted membranes increased from 107.4° to 114.4° and from 101.6° to 118.8°, respectively (Figure 3(d)). It is possible to deduce that more silane grafted onto the membrane at higher concentration, which made the surface more hydrophobic (Hamzah & Leo 2017; Thi My Hanh *et al.* 2022).

To make the PVDF hollow fiber surface more hydrophobic, the following conditions were chosen: plasma treatment of 300 W for 2 min under air and then grafted with 1 wt% MTCS or PTCS solution.

3.2. Physicochemical characterization

The pristine membrane – M0, plasma-treated membrane – M1, MTCS-grafted membrane – M2, and PTCS-grafted membrane – M3 were characterized using FTIR, XPS, SEM, and dynamic contact angle. The physicochemical properties of the four membranes were compared as follows.

3.2.1. FTIR spectra

In the FTIR spectra (Figure 4(a)), the main characteristic peaks of PVDF material can be found in all samples. For example, the peaks at 1,067 and 1,274 cm^{-1} can be attributed to the stretching of CF_2 (Thi My Hanh *et al.* 2022). Some new peaks can be found in the modified membranes. In the plasma-treated membrane M1, a new peak at 3,400 cm^{-1} is observed, which corresponds to –OH group created by plasma activation (Li *et al.* 2013). Bands at 1,053–983 cm^{-1} in M2 and bands at

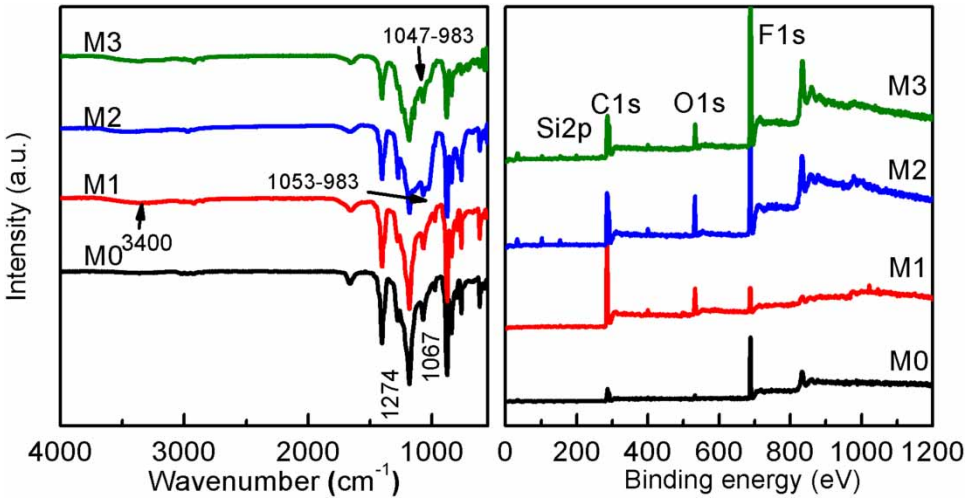

Figure 4 | FTIR spectra (a) and XPS spectra (b) of the pristine membrane M0, the plasma-treated membrane M1, MTCS-grafted membrane M2, and PTCS-grafted membrane M3.

1,047–983 cm^{-1} in M3 can be attributed to Si–O–Si bonds (Xu *et al.* 2015; Thi My Hanh *et al.* 2022). These bands prove the successful grafting of silane onto the membrane surface.

3.2.2. XPS spectra

The element compositions on the membrane surfaces were analyzed using XPS spectra (Figure 4(b) and Table 3). Compared with the pristine membrane – M0, the other three modified membranes have an obvious increase in O1s peak height and oxygen content, indicating that the oxygen-containing groups were introduced by the plasma treatment. No silicon is detected in M0 and M1, while the contents of silicon range 2.6–4.3% in M2 and M3. These changes in element composition prove the successful grafting of silane in M2 and M3.

3.2.3. Top surface morphology

The top surfaces of the four membranes were observed using SEM images (Figure 5). After the plasma treatment, M1 was more porous than M0, with more and bigger pores. These changes may be due to the plasma etching effects. However, when the plasma activation time increased to 4 min, lamellar bulges and fewer pores were found on the membrane surface (Supplementary material, Figure S2). Prolonging plasma treatment may destroy the bulk material and change the surface morphology (Xu *et al.* 2015). Unlike M1, a clear layer of polymer was covered on M2 and M3 with fewer pores. These changes prove the successful grafting of silane on M2 and M3. Comparing M2 with M3, there were more and bigger pores in M3 than M2, but the surface of M3 was more uneven with obvious microspheres on M3. These microspheres should be the self-polymerization of PTCS.

The AFM images of the four membranes are shown in Supplementary material, Figure S3, and roughness data are shown in Table 4. The roughness of M0 decreased after plasma treatment, which then increased after grafting. The roughness values (R_a and R_q) of M2 and M3 were similar.

Table 3 | Surface compositions (atomic %) of various membranes obtained from the XPS survey spectra

Membrane	C1s	O1s	F1s	Si2p
M0	53.25	5.77	38.71	–
M1	78.07	11.48	8.92	–
M2	51.72	9.38	34.60	4.29
M3	46.89	7.19	43.32	2.60

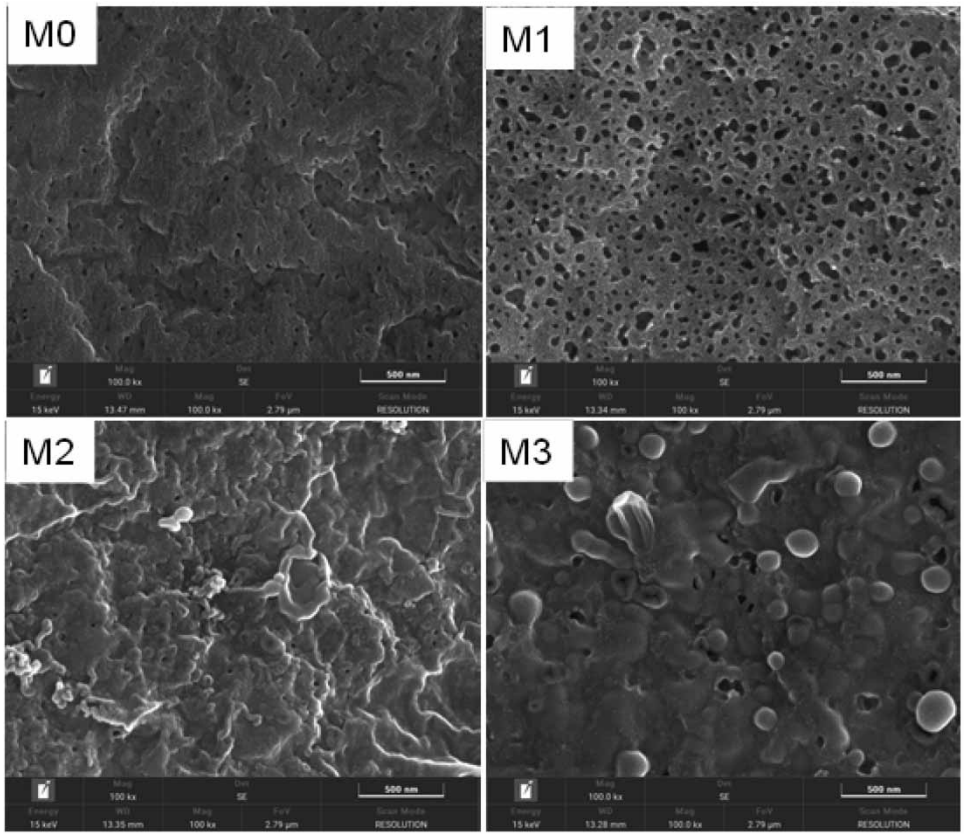

Figure 5 | Top surface SEM images of the pristine membrane M0, the plasma-treated membrane M1, MTCS-grafted membrane M2, and PTCS-grafted membrane M3.

3.2.4. Dynamic contact angle

The dynamic contact angles in 300 s were measured for M0, M2, and M3 (Figure 6). The initial WCA of M0 was less than 90°, which decreased by 23% during the following 300 s. The initial WCA values of M2 and M3 were much larger, ranging from 115° to 120°. The WCA decrease of M2 and M3 was slower, with only 7 and 3% reduction in 300 s. The WCA data indicate that the modified membranes should have stronger anti-wetting properties. M3 had a larger initial WCA and slower WCA decrease rate than M2.

3.2.5. Pore size and porosity

The bulk pore size and porosity of the membranes are listed in Table 4. Compared with the pristine membrane M0, M1 had a larger pore size of 0.395 μm. M1 and M0 showed similar porosity of 79.22–80.59%. These results are different from the changes of surface pore observed in the SEM images that an obvious increase in pore size and porosity was found in M1 (Figure 5). The plasma treatment mainly affects the top surface of the membrane and has little effect on the bulk material (Boulares-Pender *et al.* 2013; Lee *et al.* 2019).

Table 4 | Characteristics of the PVDF hollow fiber membrane (M0–M3) after modification

	AFM data					
Membrane	**R_q (nm)**	**R_a (nm)**	**Mean pore size (μm)**	**Porosity (%)**	**LEPw (bar)**	**Tensile stress (MPa)**
M0	29.8 ± 2.8	23.2 ± 2.1	0.354	80.59	1.2	3.29
M1	24.6 ± 5.5	19.2 ± 4.4	0.395	79.22	0.8	3.48
M2	43.1 ± 6.1	31.0 ± 1.7	0.284	70.13	>2.0	3.33
M3	42.0 ± 10.0	33.1 ± 7.8	0.331	78.67	>2.0	3.24

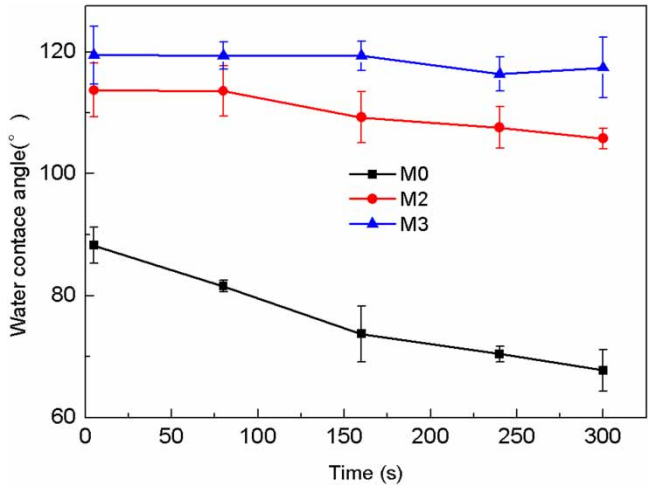

Figure 6 | Dynamic contact angle of the pristine membrane M0, the plasma-treated membrane M1, MTCS-grafted membrane M2, and PTCS-grafted membrane M3.

The grafted membranes M2 and M3 showed smaller pore sizes and lower porosity, especially higher reduction for M2. Combined with the surface changes in SEM images, it can be deduced that the silane grafting not only covered the surface pores, but also blocked the bulk pores. The decrease in pore size and porosity in M2 and M3 may cause flux reduction in the MD process (Hamzah & Leo 2017; Madalosso *et al.* 2021).

3.2.6. LEPw

LEPw represents the minimum pressure of water penetration into the membrane pores. The membrane with larger LEPw is supposed to run a longer time before wetting (Madalosso *et al.* 2021). The LEPw of the pristine membrane M0 was 1.2 bar. The modified membranes M2 and M3 had larger LEPw of >2.0 bar than M0. LEPw is strongly correlated with the WCA and pore size. M2 and M3 had larger WCAs and smaller pore sizes than M0, which led to the increase of LEPw. Conversely, the plasma-treated membrane M1 had smaller WCA and bigger surface pore size. Thus, the LEPw of M1 was the lowest, only 0.8 bar. The LEPw data indicate that M2 and M3 may show better anti-wetting properties.

3.2.7. Tensile strength

The mechanical properties are determined by tensile strength, which is an important factor showing the stiffness of the hollow fibers. The tensile strength of all membranes ranged from 3.24 to 3.48 MPa (Table 4). No significant differences in the tensile strength were observed among all the membranes. It indicates that the plasma treatment and silane grafting would not change the stiffness of the PVDF hollow fibers.

3.3. DCMD performance

3.3.1. Flux permeation and salt rejection

The water flux and salt rejection during the 8 h DCMD test treating 20 $g \cdot L^{-1}$ of NaCl solution are shown in Figure 7. The water flux values were 11.4, 7.5, and 4.3 $kg \cdot m^{-2} \cdot h^{-1}$ for M0, M2, and M3, respectively (Figure 7(a)). Compared with M0, the water flux decreased by 35 and 62% for M2 and M3, respectively. The flux reduction was consistent with the reduction of pore size and porosity (Hamzah & Leo 2017). The flux of M3 is only 57% of M2. This result is inconsistent with their physicochemical properties that M3 has higher porosity and hydrophobicity than M2. PTCS-grafted membrane seems to be denser with microspheres on top, while MTCS-grafted membrane is more evenly distributed on M2. The uneven distribution of PTCS grafting appeared to show lower flux. The flux of all three membranes remained steady during the 8-h run, indicating that membrane wetting did not happen yet.

The salt rejection of M0 kept steady at around 99.40%, which increased to 99.95 and 99.60% for M2 and M3, respectively (Figure 7(b)). High and stable salt rejection was found in M2, which may be attributed to the higher hydrophobicity and

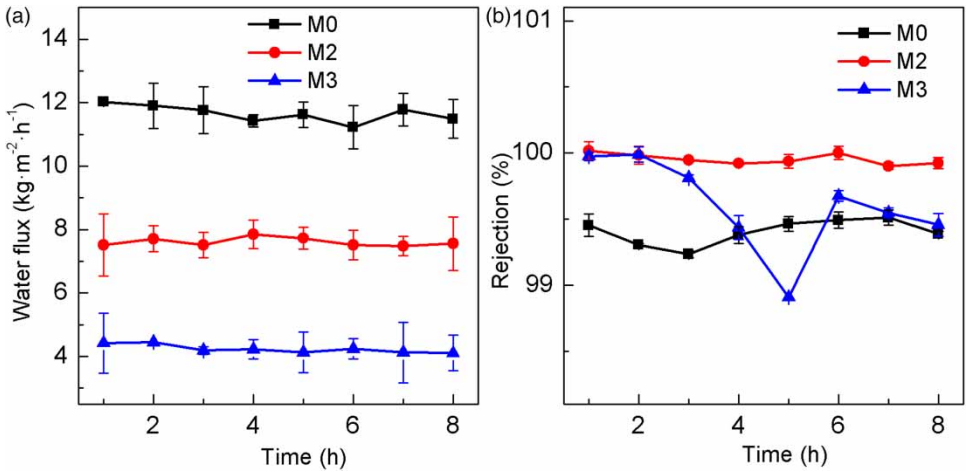

Figure 7 | Water flux (a) and salt rejection of the pristine membrane M0, MTCS-grafted membrane M2, and PTCS-grafted membrane M3 during the DCMD test of treating 20 g·L^{-1} of NaCl solution.

smaller pores. Both water flux and salt rejection data show that M2 had better DCMD performance than M3. These data are in the range of previous reports that the water flux of PVDF hollow fibers ranged 5–15 kg·m^{-2}·h^{-1} with salt rejections above 99% during the MD process (Xu *et al.* 2015; Madalosso *et al.* 2021).

3.3.2. Anti-fouling performance

The anti-fouling properties of the three membranes were investigated using the humic acid solution as the feed in a 20-h DCMD process. The water flux of the pristine membrane M0 stayed around 11 kg·m^{-2}·h^{-1} in the first 6 h, and then kept decreasing to 4 kg·m^{-2}·h^{-1} during the following 14 h, with a flux reduction of 65%. Meanwhile, the salt rejection was above 98% during the first 6 h, and then kept decreasing to below 92% at the end of the experiment (Figure 8). Membrane fouling in M0 became serious after 6 h of running, which led to the reduction of water flux and salt rejection.

Different from M0, the modified membranes M2 and M3 showed steadier water flux and salt rejection during the whole 20 h. The flux reductions were only 13 and 3% for M2 and M3, respectively. The salt rejection of M2 and M3 was kept steady above 99.5% during the whole process. These data indicate that the fouling on M2 and M3 is less serious than M0.

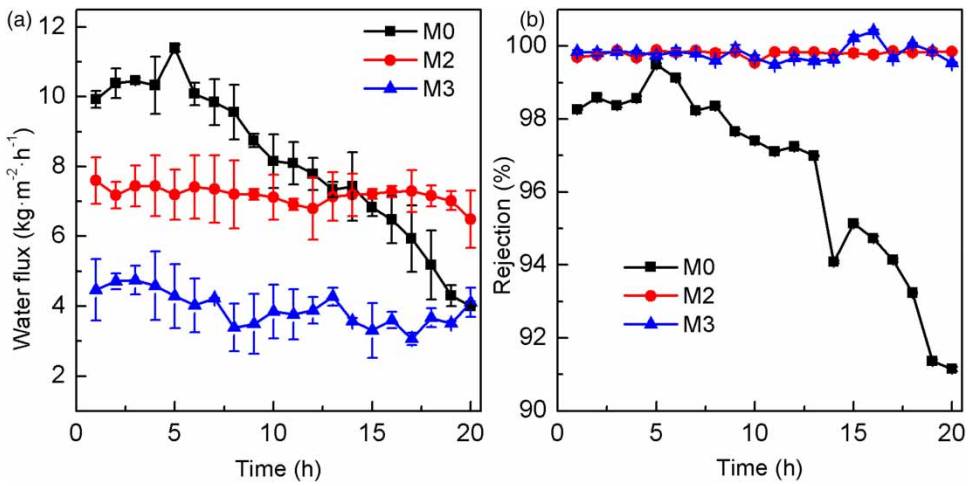

Figure 8 | Water flux (a) and salt rejection (b) of the pristine membrane M0, MTCS-grafted membrane M2, and PTCS-grafted membrane M3 during the fouling test with a feed solution of 30 mg·L^{-1} of humic acid and 35 g·L^{-1} of NaCl.

Table 5 | Change of membrane properties before and after DCMD

Membrane	WCA (°)		FRR (%)	Salt rejection (%)
	Before DCMD	After DCMD		
M0	88.62	75.07	4.75	0
M2	112.37	89.90	100	99.83
M3	116.40	98.61	100	99.79

After the 20 h of fouling test, the membranes were flushed with deionized water and tested using 20 g·L^{-1} of NaCl solution. The FRR achieved 100% for M2 and M3, while less than 5% for M0. The salt rejections were around 99.8% for M2 and M3, but no salt rejection was found with M0 (Table 5). The foulants on M2 and M3 can be easily flushed away, which was not the case for M0. The reversible fouling on M2 and M3 should be just on the membrane surface, while the irreversible fouling on M0 should be attributed to the fouling on the surface and in pores. The foulants on M0 caused the membrane wetting and resulted in bad DCMD performance.

The WCAs of all membranes decreased after the fouling test. It is usually considered that membranes with a contact angle greater than 90° are hydrophobic, while membranes with a contact angle less than 90° are hydrophilic (Duong *et al.* 2018). The fouled M0 became hydrophilic with the WCA dropping to 75°. The fouled M2 and M3 were still hydrophobic with WCAs nearly or larger than 90°. The humic acid fouling on the membrane surface caused reduction in the WCAs. More humic acid accumulated on the membrane M0, causing a darker colored surface of M0 than M2 and M3 (Supplementary material, Figure S4).

Therefore, the modified membrane showed better anti-fouling properties than the pristine membrane. However, the flux reduction after grafting should be paid attention to, and further optimization on the grafting needs to be carried out.

4. CONCLUSIONS

In this study, the hydrophobic modification of the PVDF hollow fiber membrane was carried out by plasma activation and grafting of MTCS and PTCS. The XPS, FTIR, and SEM data proved the successful grafting of silane onto the membrane surface. To achieve a more hydrophobic surface, the optimized conditions included plasma treatment of 300 W for 2 min under air and then grafted with 1 wt% MTCS or PTCS solution. The hydrophobicity of the modified membranes increased with WCA increasing from 88° to 112°–116°. Meanwhile, the pore size and porosity decreased after grafting.

These property changes complied with the decrease of water flux and increase of salt rejection during the DCMD test. The water flux decreased by 35–65% for the modified membranes during DCMD test of treating 20 g·L^{-1} of NaCl, while the rejection increased from 99.4% of the pristine membrane to 99.6–99.9% of the grafted membranes. However, during the fouling test, the modified membrane showed more excellent anti-fouling properties. The pristine membrane had serious fouling with significant flux and rejection reduction, whereas the modified membranes showed steady water flux and rejections, and had 100% flux recovery after flushing.

Plasma activation and grafting of MTCS is an effective way to hydrophobically modify PVDF hollow fibers, which show excellent anti-fouling properties. But the flux reduction should be further improved.

ACKNOWLEDGEMENTS

This work was supported by the National Natural Science Foundation of China [NSFC U 1867208] and LingChuang Research Project of China National Nuclear Corporation.

DATA AVAILABILITY STATEMENT

All relevant data are included in the paper or its Supplementary Information.

CONFLICT OF INTEREST

The authors declare there is no conflict.

REFERENCES

Boulares-Pender, A., Thomas, I., Prager, A. & Schulze, A. 2013 Surface modification of polyamide and poly(vinylidene fluoride) membranes. *Journal of Applied Polymer Science* **128** (1), 322–331.

Deng, L., Liu, K., Li, P., Sun, D., Ding, S., Wang, X. & Hsiao, B. S. 2020 Engineering construction of robust superhydrophobic two-tier composite membrane with interlocked structure for membrane distillation. *Journal of Membrane Science* **598**, 117813.

Duong, H. C., Chuai, D., Woo, Y. C., Shon, H. K., Nghiem, L. D. & Sencadas, V. 2018 A novel electrospun, hydrophobic, and elastomeric styrene-butadiene-styrene membrane for membrane distillation applications. *Journal of Membrane Science* **549**, 420–427.

Eykens, L., De Sitter, K., Dotremont, C., Pinoy, L. & Van der Bruggen, B. 2017 Membrane synthesis for membrane distillation: a review. *Separation and Purification Technology* **182**, 36–51.

Gryta, M. 2021a Surface modification of polypropylene membrane by helium plasma treatment for membrane distillation. *Journal of Membrane Science* **628**, 119265.

Gryta, M. 2021b Application of polypropylene membranes hydrophilized by plasma for water desalination by membrane distillation. *Desalination* **515**, 115187.

Hamzah, N. & Leo, C. P. 2017 Membrane distillation of saline with phenolic compound using superhydrophobic PVDF membrane incorporated with TiO2 nanoparticles: separation, fouling and self-cleaning evaluation. *Desalination* **418**, 79–88.

Hamzah, N., Nagarajah, M. & Leo, C. P. 2018 Membrane distillation of saline and oily water using nearly superhydrophobic PVDF membrane incorporated with SiO2 nanoparticles. *Water Science and Technology* **78** (12), 2532–2541.

Hou, D., Wang, J., Qu, D., Luan, Z., Zhao, C. & Ren, X. 2009 Preparation of hydrophobic PVDF hollow fiber membranes for desalination through membrane distillation. *Water Science and Technology* **59** (6), 1219–1226.

Hou, D., Zhang, L., Wang, Z., Fan, H., Wang, J. & Huang, H. 2015 Humic acid fouling mitigation by ultrasonic irradiation in membrane distillation process. *Separation and Purification Technology* **154**, 328–337.

Jeong, S., Shin, B., Jo, W., Kim, H.-Y., Moon, M.-W. & Lee, S. 2016 Nanostructured PVDF membrane for MD application by an O-2 and CF4 plasma treatment. *Desalination* **399**, 178–184.

Kang, G. D. & Cao, Y. M. 2014 Application and modification of poly(vinylidene fluoride) (PVDF) membranes – a review. *Journal of Membrane Science* **463**, 145–165.

Kawakami, R., Yoshitani, Y., Mitani, K., Niibe, M., Nakano, Y., Azuma, C. & Mukai, T. 2020 Effects of air-based nonequilibrium atmospheric pressure plasma jet treatment on characteristics of polypropylene film surfaces. *Applied Surface Science* **509**, 144910.

Kravets, L. I., Altynov, V. A., Yarmolenko, M. A., Gainutdinov, R. V., Satulu, V., Mitu, B. & Dinescu, G. 2022 Deposition of hydrophobic polymer coatings on the surface of track-etched membranes from an active gas phase. *Membranes and Membrane Technologies* **4** (2), 133–143.

Lee, H. K., Kim, W., Kim, Y. M. & Kwon, Y.-N. 2019 Surface modification of polyvinylidene fluoride membrane for enhanced wetting resistance. *Applied Surface Science* **491**, 32–42.

Li, M.-S., Zhao, Z.-P., Li, N. & Zhang, Y. 2013 Controllable modification of polymer membranes by long-distance and dynamic low-temperature plasma flow: treatment of PE hollow fiber membranes in a module scale. *Journal of Membrane Science* **427**, 431–442.

Liu, L., Shen, F., Chen, X., Luo, J., Su, Y., Wu, H. & Wan, Y. 2016 A novel plasma-induced surface hydrophobization strategy for membrane distillation: etching, dipping and grafting. *Journal of Membrane Science* **499**, 544–554.

Madalosso, H. B., Machado, R., Hotza, D. & Marangoni, C. 2021 Membrane surface modification by electrospinning, coating, and plasma for membrane distillation applications: a state-of-the-art review. *Advanced Engineering Materials* **23** (6), 2001456.

Mousavi, S. A., Arab Aboosadi, Z., Mansourizadeh, A. & Honarvar, B. 2021 Modification of porous polyetherimide hollow fiber membrane by dip-coating of Zonyl (R) BA for membrane distillation of dyeing wastewater. *Water Science and Technology* **83** (12), 3092–3109.

Ray, S. S., Bakshi, H. S., Dangayach, R., Singh, R., Deb, C. K., Ganesapillai, M., Chen, S.-S. & Purkait, M. K. 2020 Recent developments in nanomaterials-Modified membranes for improved membrane distillation performance. *Membranes* **10** (7), 140–168.

Sharma, A. K., Juelfs, A., Colling, C., Sharma, S., Conover, S. P., Puranik, A. A., Chau, J., Rodrigues, L. & Sirkar, K. K. 2021 Porous hydrophobic-hydrophilic composite hollow fiber and flat membranes prepared by plasma polymerization for direct contact membrane distillation. *Membranes* **11** (2), 120–135.

Teoh, M. M. & Chung, T.-S. 2009 Membrane distillation with hydrophobic macrovoid-free PVDF–PTFE hollow fiber membranes. *Separation and Purification Technology* **66** (2), 229–236.

Thi My Hanh, L., Nuisin, R., Mongkolnavin, R., Painmanakul, P. & Sairiam, S. 2022 Enhancing dye wastewater treatment efficiency in ozonation membrane contactors by chloro- and fluoro-organosilanes' functionality on hydrophobic PVDF membrane modification. *Separation and Purification Technology* **288**, 120711.

Tran, T. T. V., Nguyen, C. H., Lin, W.-C. & Juang, R.-S. 2021 Improved stability of a supported liquid membrane process via hydrophobic modification of PVDF support by plasma activation and chemical vapor deposition. *Separation and Purification Technology* **277**, 119615.

Xu, W.-T., Zhao, Z.-P., Liu, M. & Chen, K.-C. 2015 Morphological and hydrophobic modifications of PVDF flat membrane with silane coupling agent grafting via plasma flow for VMD of ethanol-water mixture. *Journal of Membrane Science* **491**, 110–120.

Yan, Z., Jiang, Y., Liu, L., Li, Z., Chen, X., Xia, M., Fan, G. & Ding, A. 2021 Membrane distillation for wastewater treatment: a mini review. *Water* **13** (24), 3480–3507.

Yang, X., Wang, R., Shi, L., Fane, A. G. & Debowski, M. 2011 Performance improvement of PVDF hollow fiber-based membrane distillation process. *Journal of Membrane Science* **369** (1–2), 437–447.

Zhang, Y., Wang, X., Cui, Z., Drioli, E., Wang, Z. & Zhao, S. 2017 Enhancing wetting resistance of poly(vinylidene fluoride) membranes for vacuum membrane distillation. *Desalination* **415**, 58–66.

Zhang, W., Hu, B., Wang, Z. & Li, B. 2021 Fabrication of omniphobic PVDF composite membrane with dual-scale hierarchical structure via chemical bonding for robust membrane distillation. *Journal of Membrane Science* **622**, 119038.

First received 13 February 2023; accepted in revised form 13 May 2023. Available online 29 May 2023